Lymphatic endothelial cell sphingosine kinase activity is required for lymphocyte egress and lymphatic patterning

Trung H.M. Pham,[1] Peter Baluk,[2] Ying Xu,[1] Irina Grigorova,[1] Alex J. Bankovich,[1] Rajita Pappu,[3] Shaun R. Coughlin,[3] Donald M. McDonald,[2] Susan R. Schwab,[4] and Jason G. Cyster[1]

[1]Howard Hughes Medical Institute and Department of Microbiology and Immunology, [2]Department of Anatomy, and [3]Cardiovascular Research Institute, University of California, San Francisco, San Francisco, CA 94143
[4]Skirball Institute, New York University, New York, NY 10016

<div style="writing-mode: vertical">The Journal of Experimental Medicine</div>

Lymphocyte egress from lymph nodes (LNs) is dependent on sphingosine–1–phosphate (S1P), but the cellular source of this S1P is not defined. We generated mice that expressed *Cre* from the lymphatic vessel endothelial hyaluronan receptor 1 (*Lyve-1*) locus and that showed efficient recombination of *loxP*–flanked genes in lymphatic endothelium. We report that mice with *Lyve-1* CRE–mediated ablation of sphingosine kinase (*Sphk*) *1* and lacking *Sphk2* have a loss of S1P in lymph while maintaining normal plasma S1P. In *Lyve-1 Cre+ Sphk*–deficient mice, lymphocyte egress from LNs and Peyer's patches is blocked. Treatment with pertussis toxin to overcome Gαi–mediated retention signals restores lymphocyte egress. Furthermore, in the absence of lymphatic *Sphks*, the initial lymphatic vessels in nonlymphoid tissues show an irregular morphology and a less organized vascular endothelial cadherin distribution at cell–cell junctions. Our data provide evidence that lymphatic endothelial cells are an in vivo source of S1P required for lymphocyte egress from LNs and Peyer's patches, and suggest a role for S1P in lymphatic vessel maturation.

CORRESPONDENCE
Jason G. Cyster:
Jason.Cyster@ucsf.edu

Abbreviations used: BEC, blood endothelial cell; FRC, fibroblastic reticular cell; LEC, lymphatic endothelial cell; LYVE-1, lymphatic vessel endothelial hyaluronan receptor 1; OB, oligomer-B; PTX, pertussis toxin; S1P, sphingosine-1-phosphate; Sphk, sphingosine kinase; VE-cadherin, vascular endothelial cadherin.

Lymphocyte egress from LNs into lymph requires lymphocyte-intrinsic sphingosine-1-phosphate receptor 1 (S1P1), a G protein–coupled receptor (Matloubian et al., 2004). S1P1 promotes migration into exit structures, the lymphatic vessel endothelial hyaluronan receptor 1+ (LYVE-1+) cortical sinuses of the LNs, within which lymphocytes may be captured by lymphatic flow and transported to the efferent lymph (Pham et al., 2008; Grigorova et al., 2009; Sinha et al., 2009). S1P is normally low in the lymphoid tissue and abundant in blood and lymph, and disruption of this S1P gradient results in an egress block (Schwab et al., 2005; Pappu et al., 2007). However, despite its importance for lymphocyte egress, the cellular source of lymph S1P remains unknown (Schwab and Cyster, 2007).

S1P production is dependent on sphingosine kinase (Sphk) 1 and 2, enzymes that are expressed in most eukaryotic cell types (Kono et al., 2008). Recent work has demonstrated that red blood cells are a major source of plasma S1P, whereas all lymph S1P and ∼5% of plasma

S1P are supplied by a distinct, radiation-resistant source (Pappu et al., 2007). In vitro studies have shown that blood endothelial cells (BECs) can act as a source of S1P (Venkataraman et al., 2008). However, it has not been determined whether endothelial cells are an important source of S1P in vivo.

Lymphatic endothelial cells (LECs) arise from the venous endothelium during embryonic development at around embryonic day (E) 9–9.5, when a subpopulation of endothelial cells of the anterior cardinal vein commit to the lymphatic lineage by turning on *Prox1* expression (Karpanen and Alitalo, 2008). LYVE-1 is the earliest expressing and one of the most specific and widely used markers for LECs (Karpanen and Alitalo, 2008; Oliver and Srinivasan, 2008).

Mice lacking *Sphk1* and *Sphk2* die in utero between E11.5–13.5 because of blood vascular

JEM

defects (Mizugishi et al., 2005). In vitro, stimulation of BECs with S1P increases localization of vascular endothelial cadherin (VE-cadherin) at cell–cell junctions and induces tubular morphogenesis (Lee et al., 1999). Recently, S1P was demonstrated to promote tubular formation of human dermal LECs in vitro and lymphangiogenesis in Matrigel in vivo (Yoon et al., 2008). However, whether S1P signaling normally plays a role in the development of the lymphatic system is not known.

In this report, by examining mice that lack *Sphk2* and have *Sphk1* conditionally deleted by a CRE recombinase expressed from the *Lyve-1* locus, we provide evidence that LECs are the major source of lymph S1P. Lymphatic *Sphk*-deficient mice experienced a block of T and B cell egress from LNs. Additionally, lymphatic *Sphk*-deficient mice displayed altered initial lymphatic vessel morphology and junctional VE-cadherin patterning in the trachea and diaphragm.

RESULTS AND DISCUSSION
Specificity of *Lyve–1* CRE–mediated gene deletion
To achieve ablation of *loxP*-flanked genes in LECs, we generated a knockin mouse line in which an *EGFP-hCre* transgene preceded by an internal ribosomal entry site was inserted into the 3′ untranslated region of the *Lyve-1* gene (Fig. S1, A and B). Immunofluoresence analysis of tissue from *Lyve-1 EGFP-hCre*+ mice showed selective GFP staining in the nuclei of LYVE-1+ cells (Fig. S1 C). In the absence of antibody staining, however, the eGFP fluorescence was not readily detected, and for simplicity we refer to the knockin mice as *Lyve-1 Cre*+ mice. To determine the efficiency and specificity of *Lyve-1 Cre*–mediated gene deletion, *Lyve-1 Cre*+ mice were intercrossed to mice carrying YFP preceded by a floxed transcriptional stop in the Rosa26 locus (Srinivas et al., 2001). Activation of reporter expression was examined in LNs. By flow cytometric analysis, we identified LN LECs as CD45− CD31hi gp38 (podoplanin)hi cells (Fig. 1 A; Link et al., 2007). To confirm the identity of these cells as LECs, we further demonstrated that they express high amounts of surface LYVE-1 (Fig. 1 A) as compared with CD45− CD31hi gp38lo BECs, CD45− CD31lo gp38hi fibroblastic reticular cells (FRCs), and other CD45− LN stromal cells. When analyzed for reporter expression, >90% of LECs were YFP+ (Fig. 1 B), indicating efficient CRE-mediated gene deletion in these cells. A varying fraction of BECs was also positive for YFP reporter expression, probably because of the differential expression of LYVE-1 in subsets of BECs that has been observed during embryonic development (Gordon et al., 2008). In contrast, few FRCs were YFP+. We also observed that a fraction of CD45+ cells (42.4 ± 6.8%), including lymphocytes (41.8 ± 5.8%) and myeloid cells (42.9 ± 2.4%), were YFP+, suggesting that there is some Cre activity in hematopoietic precursor cells. It will be valuable in future studies to examine hematopoietic precursors for LYVE-1 expression.

Immunofluorescence analysis of LN tissues obtained from *Lyve-1 Cre*+ YFP reporter mice that had been lethally irradiated and reconstituted with wild-type BM showed extensive overlap between YFP and LYVE-1 immunoreactivity (Fig. 1 C). In particular, the cells lining cortical sinusoids, identified by their LYVE-1 staining and location in the T cell zone, showed

YFP expression (Fig. 1 C). YFP was variably observed in non–LYVE-1+ endothelial cells, as well as some other cells that are likely radiation-resistant lymphocytes. YFP was also observed in LYVE-1+ lymphatic vessels in the ear dermis and small intestine (Fig. S2, A and B). Collectively, these findings indicate the *Lyve-1 Cre*+ mice exhibit efficient recombination of a floxed gene element in LYVE-1+ cells within lymphoid and nonlymphoid tissues.

S1P metabolic enzyme expression by LECs
By quantitative PCR analysis we detected selective expression of *Lyve-1* and *Prox1* in the isolated LN LEC population, confirming their lymphatic identity (Fig. 1 D). LECs expressed *Sphk1* and *Sphk2* abundantly compared with spleen cells (Fig. 1 D). Reciprocally, analysis of enzymes that degrade S1P revealed that LECs have a lower abundance of transcripts for S1P lyase, lipid phosphate phosphatase 3, and S1P-phosphatase 1 than one or more of the other cell types analyzed (Fig. 1 D). Recently, SPNS2 was implicated as an S1P transporter in zebrafish (Osborne et al., 2008; Kawahara et al., 2009). Transcripts for the mouse SPNS2 orthologue were abundantly expressed in LECs (Fig. 1 D). Thus, LN LECs have a transcriptional profile consistent with their functioning as a source of extracellular S1P.

Ablation of lymph S1P by conditional deletion of *Sphk1* in *Sphk2* null mice
To test the role of LYVE-1+ cells in generating lymph S1P, we intercrossed *Lyve-1 Cre*+ mice with animals carrying floxed and null alleles of *Sphk1* and null alleles of *Sphk2*. Flow cytometric analysis of lymphocytes in the lymph of *Lyve-1 Cre*+ *Sphk1*f/− or f/f *Sphk2*−/− mice showed high surface S1P1 as compared with controls, which had undetectable amounts of receptor (Fig. 2 A). Lymphocyte S1P1 is very sensitive to S1P-induced down-modulation, and 1 nM S1P down-modulates S1P1 on mature thymocytes (Schwab et al., 2005). Thus, the high surface S1P1 on lymphocytes in the lymph suggested a marked reduction from the normal 100–300-nM lymph S1P concentration (Pappu et al., 2007). In contrast, lymphocytes from the blood of lymphatic *Sphk*-deficient and control mice both had undetectable surface S1P1 (Fig. 2 A), consistent with blood S1P being maintained mostly by red blood cells (Pappu et al., 2007). Using a sensitive S1P bioassay in which S1P concentration is measured by the extent of Flag-tagged S1P1 receptor down-modulation in a cell line (Schwab et al., 2005; Pappu et al., 2007), the lymphatic *Sphk*-deficient mice had undetectable amounts of S1P in lymph, indicating that levels were at least 50-fold lower than in control mice (Fig. 2 B). There was no difference in blood S1P abundance between lymphatic *Sphk*-deficient and control mice (Fig. 2 B).

LYVE-1–expressing macrophages are not a significant source of lymph S1P
Besides LECs, a subset of macrophages has been suggested to express LYVE-1 (Jackson, 2004). To determine the radiation

sensitivity of LYVE-1⁺ LN macrophages and test if they made a contribution to lymph S1P, we performed BM chimera studies, reconstituting CD45.2⁺ lymphatic *Sphk*-deficient mice with CD45.1⁺ wild-type BM. Using a gating scheme previously used to identify LN macrophage subsets (Jakubzick et al., 2008), CD11b^{hi} CD11c^{med} and CD11b^{hi} CD11c^{lo} cell subsets were found to express LYVE-1 (Fig. 3, A and B). Importantly, these LYVE-1⁺ macrophage subsets exhibited >85% chimerism (Fig. 3 C). There was similarly high replacement of all the myeloid cell subsets (Fig. 3 C) as well as
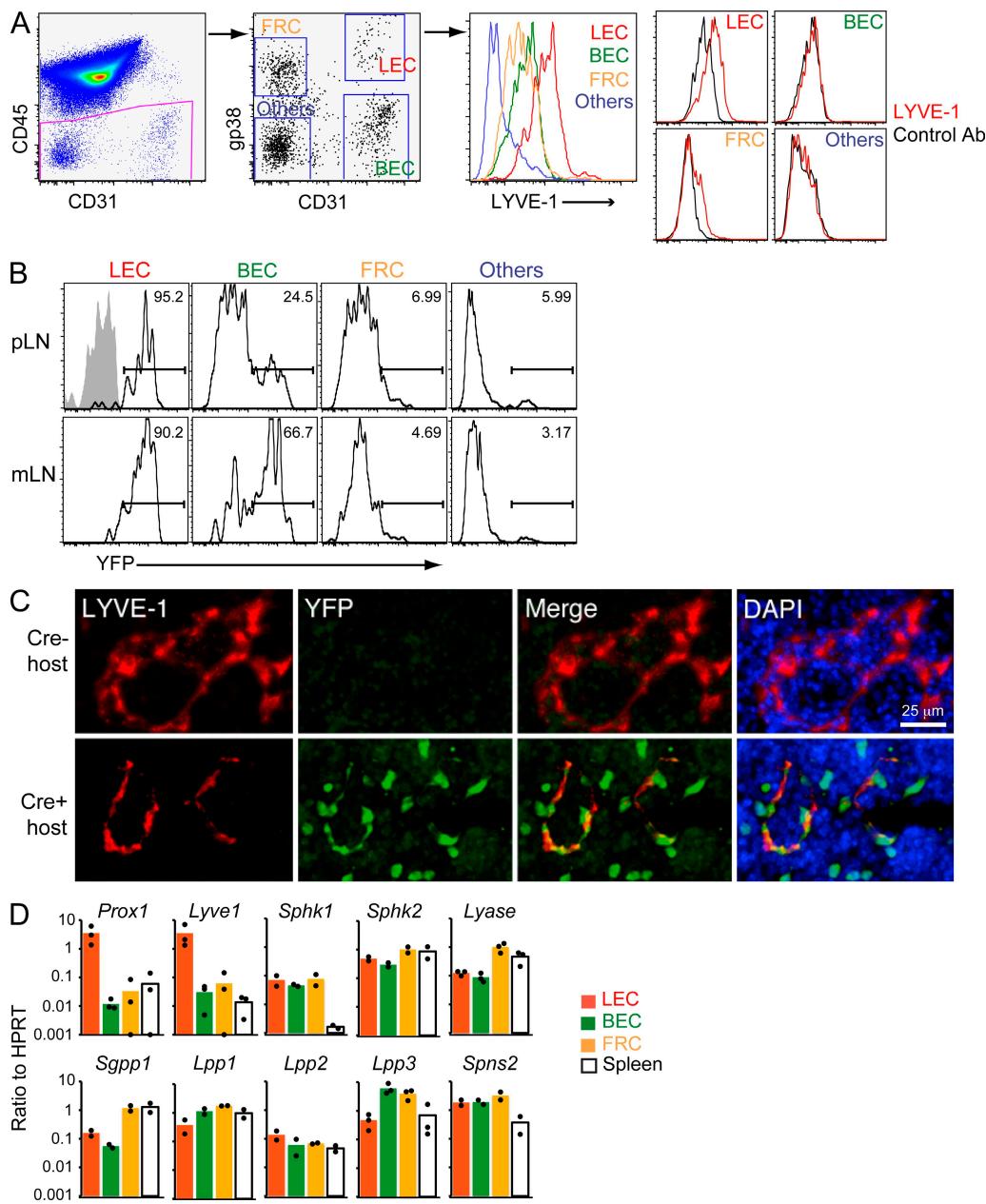
Figure 1. Efficiency of *Lyve-1* CRE–mediated gene deletion and S1P metabolic enzyme expression in LECs. (A) Isolation and identification of LECs. LNs were minced and digested as detailed in Materials and methods. CD31 and gp38 expression allows separation of LECs from other CD45⁻ cells: FRCs, BECs, and double-negative stromal cells (Others). (left plot) LYVE-1 on indicated populations; (right plots) Control stains for each cell type. (B) Flow cytometric analysis of YFP in cells isolated from LNs of *Lyve-1 Cre*⁺ Rosa26-YFP reporter mice (percentages are shown). The four cell populations are gated according to the scheme in A. Peripheral LNs (pLN; axillary, brachial, and inguinal nodes) and mesenteric LNs (mLN) are shown. The shaded histogram represents Cre-negative cells. (C) Immunofluorescence analysis of YFP in LNs of *Lyve-1 Cre*⁺ or Rosa26-YFP mice that had been reconstituted with wild-type BM. Fixed LN sections were stained as indicated. Data in A–C are representative of at least three experiments with one to two mice of each type per experiment. (D) Quantitative RT-PCR analysis of S1P metabolic genes in cells sorted from a pool of peripheral and mesenteric LNs using the scheme in A and from spleen tissue or splenic B cells. Data are representative of three separate sorts with 10–15 mice in each sort, with each gene expression measured at least twice. Bars represent means.

lymphocytes (not depicted). In these BM chimeras, lymph S1P was reduced to the same extent observed in nonchimeric *Sphk*-deficient animals, as indicated by the presence of surface S1P1 on T cells in the lymph (Fig. 3 D) and by S1P bioassay (Fig. 3 E). These experiments suggest that hematopoietic cells within LNs, including the LYVE-1–expressing macrophage subpopulations, do not make a significant contribution to lymph S1P.

Impaired lymphocyte egress in lymphatic *Sphk*-deficient mice
Flow cytometric analysis of lymph isolated from the cysterna chyli of lymphatic *Sphk*-deficient mice revealed that T and B lymphocyte numbers were markedly reduced, in some cases up to 50-fold (Fig. 4 A), indicating that egress from LNs was strongly reduced. We detected a similar extent of egress impairment in lymphatic *Sphk*-deficient mice that had been reconstituted with wild-type BM (Fig. S2 C). There was also a decrease in lymphocyte numbers in the circulation and the spleen (Fig. 4, B and C). Because blood S1P levels were normal in lymphatic *Sphk*-deficient mice, lymphocytes presumably could egress from the spleen and traffic to the LNs, where their egress is impaired. Interestingly, we did not observe an expansion of the lymphocyte compartment in the LNs but saw a consistent reduction of T cell numbers (Fig. 4 D). Concomitantly, there was an accumulation of naive T cells in the Peyer's patches (Fig. 4 E). We observed a larger increase of surface S1P1 on naive T cells recovered from Peyer's

patches of lymphatic *Sphk*-deficient mice as compared with the increase exhibited in the LNs, suggesting a more complete loss of S1P availability in the Peyer's patches (Fig. 4 F). The reduced T cell numbers in LNs cannot be adequately accounted for by the accumulation in Peyer's patches, and we did not find an accumulation of T cells in the liver or lung (Fig. S2 D). The reduction in LN T cells may reflect a requirement for T cells to recirculate between lymphoid tissues (Link et al., 2007), or possibly a more direct effect of S1P on T cells or the LN microenvironment that promotes T cell survival (Kennedy et al., 2009).

Consistent with the reduced lymphocyte numbers in the lymph, LYVE-1^{+} sinuses in lymphatic *Sphk*-deficient LNs contained almost no lymphocytes and appeared collapsed (Fig. 4 G). In contrast, LYVE-1^{+} sinuses in control LNs were extended with cells (Fig. 4 G). A similar emptying of cortical sinuses was seen 6 h after treatment of wild-type mice with the S1P1-modulating and egress-inhibiting drug FTY720 (Rosen and Goetzl, 2005; Schwab and Cyster, 2007), indicating that sinus emptying can occur rapidly and need not reflect a developmental abnormality (Fig. S2 E). Lymphatic *Sphk*-deficient animals also showed a deficiency of lymphocytes in intestinal lymphatic sinuses adjacent to and likely draining from (Azzali, 2003) Peyer's patches (Fig. 4 H). These findings provide evidence for the involvement of lymphatic-derived S1P in the earliest step of lymphocyte egress from LNs and Peyer's patches.
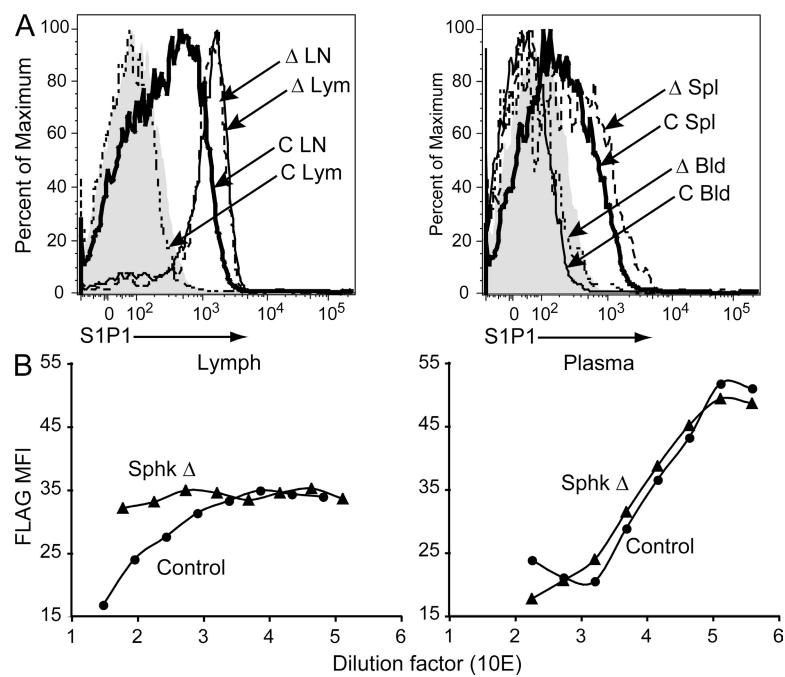
Figure 2. Ablation of lymph S1P by conditional deletion of *Sphk1* in *Sphk2*-deficient mice. (A) Flow cytometric analysis showing S1P1 on CD4^{+} CD62L^{hi} T cells from the indicated circulatory fluids and tissues. Δ indicates *Lyve-1 Cre^{+} Sphk1[f/- or f/f] Sphk2^{-/-}* mice; C indicates littermate control. The shaded histograms show staining with control antibody of cells from LN and blood. Bld, blood; Lym, lymph; Spl, spleen. (B) Measurement of S1P level by bioassay. Lymph fluid and plasma samples were prepared (see Materials and methods) and titrated onto WEHI231 cells expressing FLAG-S1P1. The x axis shows dilution of the samples. The y axis indicates mean fluorescence intensity (MFI) of FLAG antibody staining. Data are representative of at least five experiments with one to two mice each.

Restoration of egress in lymphatic S1P–deficient mice by pertussis toxin (PTX) treatment

When Gαi-mediated retention signals are blocked, the lymphocyte-intrinsic requirement for S1P1 during LN egress is partially overcome (Pham et al., 2008). To test whether the lymphocyte egress defect in *Lyve-1 Cre+ Sphk*-deficient mice occurs via effects on the lymphocytes, we sought to determine if inhibition of Gαi-mediated retention signaling would restore egress. Wild-type lymphocytes were treated ex vivo either with PTX or the nonenzymatic oligomer-B (OB) subunit of PTX as a control using a pulse-loading procedure that allowed treated cells to continue entry into LNs for 2–3 h after being transferred into recipient mice, before complete inhibition of Gαi (Lo et al., 2005; Pham et al., 2008). After 1 d of equilibration, the distribution of transferred cells in host animals was determined. Although the frequency of PTX-

treated T cells in lymph was about one third the frequency of OB-treated cells in the control hosts, their frequency was up to eightfold higher than that of OB-treated cells in the lymph of lymphatic *Sphk*-deficient hosts (Fig. 5, A and B). These data suggest that although egress of control (OB)-treated T cells was blocked in lymphatic *Sphk*-deficient animals, PTX-treated cells continued to exit into the lymph. Moreover, the appearance of cotransferred PTX-treated but not control cells in the lymph also makes it unlikely that the marked reduction in control cells in the lymph is caused by a loss of lymph flow through the LN. When absolute cell numbers were plotted, there was no difference in the numbers of PTX-treated T cells in lymph of control and lymphatic *Sphk*-deficient recipients, suggesting that these cells can undergo egress to a similar extent in both types of hosts (Fig. 5 C). PTX treatment also partially restored B cell egress in host
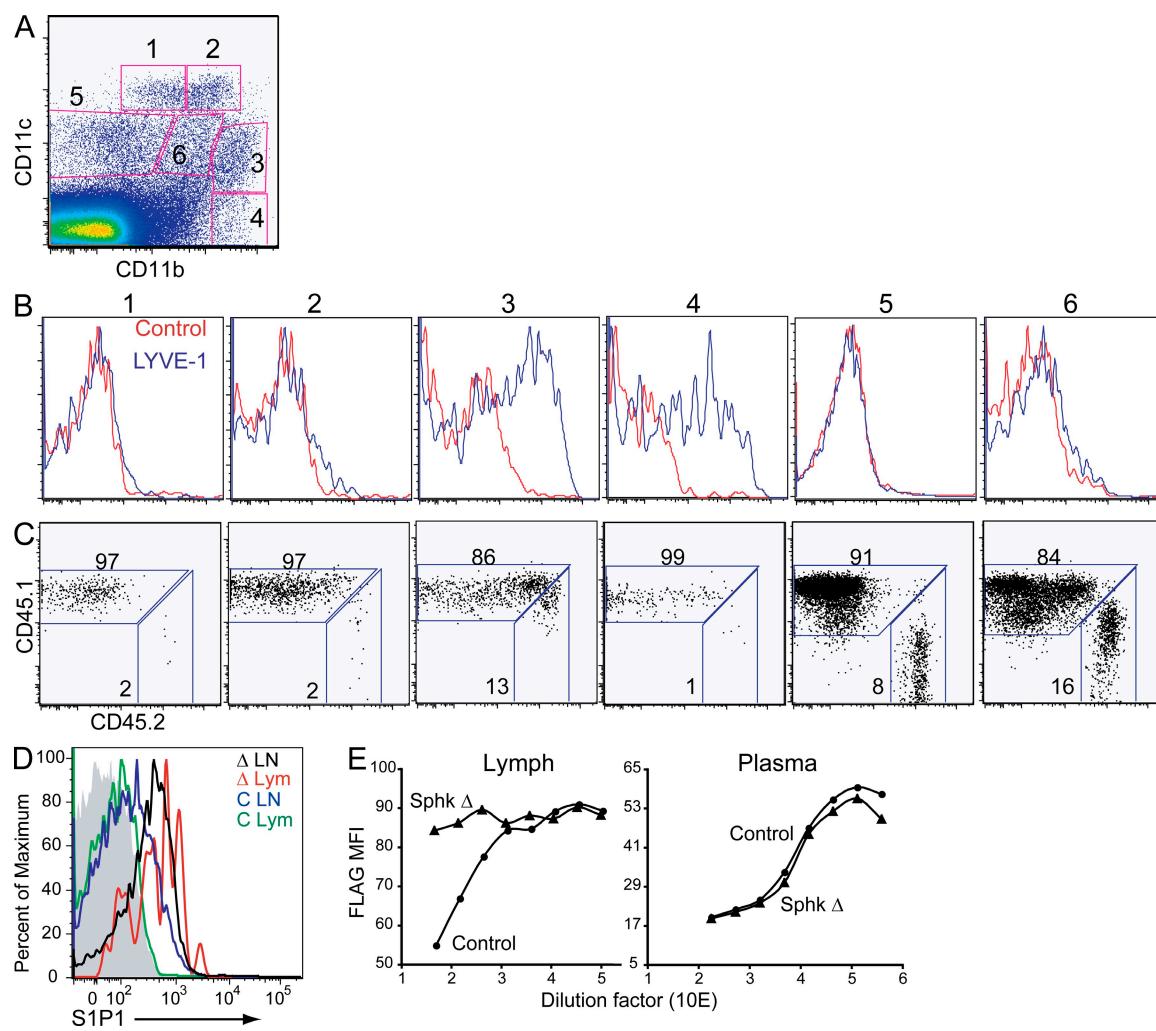

Figure 3.   Lack of contribution of myeloid cells to lymph S1P. (A) Flow cytometric analysis of enzyme-digested LN cells to detect CD11b and CD11c. (B) LYVE-1 or control antibody staining of the six cell populations shown in A. (C) The proportion of each subpopulation replaced by donor-derived cells in lethally irradiated CD45.2+ *Lyve-1 Cre+ Sphk*-deficient mice reconstituted with wild-type CD45.1+ BM. Numbers refer to the percentage of cells in the indicated gates. (D) S1P1 on CD4+ CD62Lhi T cells from the lymph and LNs of mice that had been reconstituted with wild-type BM as in C. *Sphk* Δ indicates the *Lyve-1* Cre+ Sphk-deficient host; C indicates the control host. The shaded histogram shows staining of LN cells from an FTY720-treated mouse. (E) Bioassay measurement of S1P in lymph and plasma from the chimeric mice. Data in A–E are representative of three experiments with three mice. MFI, mean fluorescence intensity.

animals deficient in lymph S1P (Fig. S3, A and B). By immu-nohistochemical analysis, OB-treated T cells were found in the LYVE-1^{+} cortical sinuses of control but not lymphatic *Sphk*-deficient mice (Fig. 5 D and Fig. S3 C). In contrast, PTX-treated cells could be identified within the cortical si-nuses of both control and lymphatic *Sphk*-deficient mice (Fig. 5 D and Fig. S3 C). Collectively, these findings support the conclusion that LEC-derived S1P acts on lymphocytes to promote localization of cells within LYVE-1^{+} sinuses and egress from LNs.

Altered lymphatic vasculature in lymphatic *Sphk*-deficient mice

Because of the established functions of S1P signaling in the development of the blood vasculature, we sought to deter-mine if ablation of lymph S1P had an effect on lymphatic vasculature. Lymphatic vessel morphology and architecture in the trachea and diaphragm have been well studied (Baluk et al., 2007), and we therefore examined these tissues. When visualized by whole-mount staining for LYVE-1, the lym-phatic vessels in the trachea of lymphatic *Sphk*-deficient
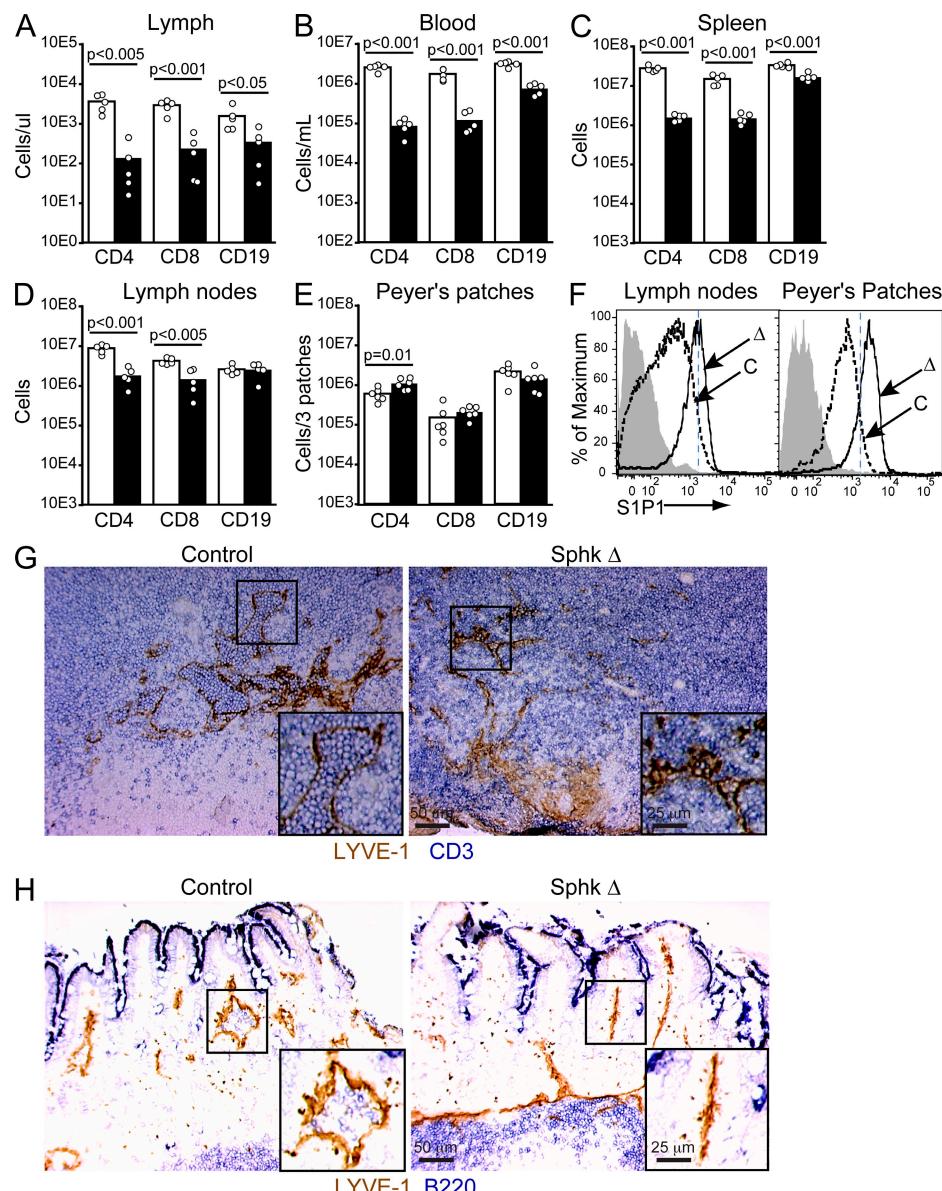
Figure 4. Impaired lymphocyte egress in *Lyve-1 Cre Sphk*-deficient mice. (A–E) Cell numbers in the indicated fluids and tissues in *Lyve-1 Cre+ Sphk*-deficient and control mice. The LN count was from a pool of two axillary, brachial, and inguinal LNs. Enumerated CD4+, CD8+, and CD19+ cells were CD62L^{hi}. Points indicate data from individual mice, and white (control mice) and black (*Sphk*-deficient mice) bars represent means. (F) S1P1 on CD4+ CD62L^{hi} T cells from the indicated tissues. Shaded histograms show staining with control antibody. The vertical dashed lines mark the peak S1P1 intensity in the LN sample to allow comparison. Data in A–F are representative of at least three experiments with one to two mice per experiment. (G and H) Immunohistochemial analysis of LNs (G) and Peyer's patches (H) stained for LYVE-1 (brown) and CD3 (blue) or B220 (blue).

discontinuous junctions at the initial lymphatics were apparent and often consisted of a series of "buttons" (Baluk et al., 2005), the junctions in the affected animals were less defined, usually being made up by fewer or more diffuse buttons (Fig. 6, B and C; and Fig. S4 C). Consistent with previous studies (Yoon et al., 2008; Sinha et al., 2009), we found that LECs expressed *S1p1*, and to a lesser extent *S1p3* (Fig. S4 D), suggesting that LECs are capable of transducing signals from extracellular S1P that mediate organization of lymphatic cell–cell junctions. Taking these findings together with earlier work, S1P may have similar actions on blood vessel and lymphatic endothelium, regulating the localization of cadherins at cell–cell junctions. LN LECs also express VE-cadherin (Pfeiffer et al., 2008), but its junctional distribution has not yet been well studied. In wild-type LNs, we observed a VE-cadherin distribution in LYVE-1+ sinuses that was less well defined than the buttons and zippers

(Baluk et al., 2005) of nonlymphoid tissue lymphatics (Fig. S4 E). In the lymphatic Sphk-deficient mice, although the LN LYVE-1+ sinuses often appeared collapsed, the VE-cadherin distribution appeared similar (Fig. S4 E). However, higher resolution approaches will be required to determine precisely how VE-cadherin is organized at LN cortical sinus cell junctions of wild-type and mutant mice.

To determine if the altered morphology of initial lymphatics in *Lyve-1 Cre+ Sphk*-deficient mice led to major defects in cell trafficking, we examined the numbers of tissue-derived DCs in skin-draining LNs. By gating on a population that contains the majority of the skin-derived DCs in the LNs (Jakubzick et al., 2008), we observed no apparent difference in the numbers of these cells in lymphatic Sphk-deficient and control mice under steady state (Fig. S4 F). In a second experiment, BM-derived DCs were transferred subcutaneously to
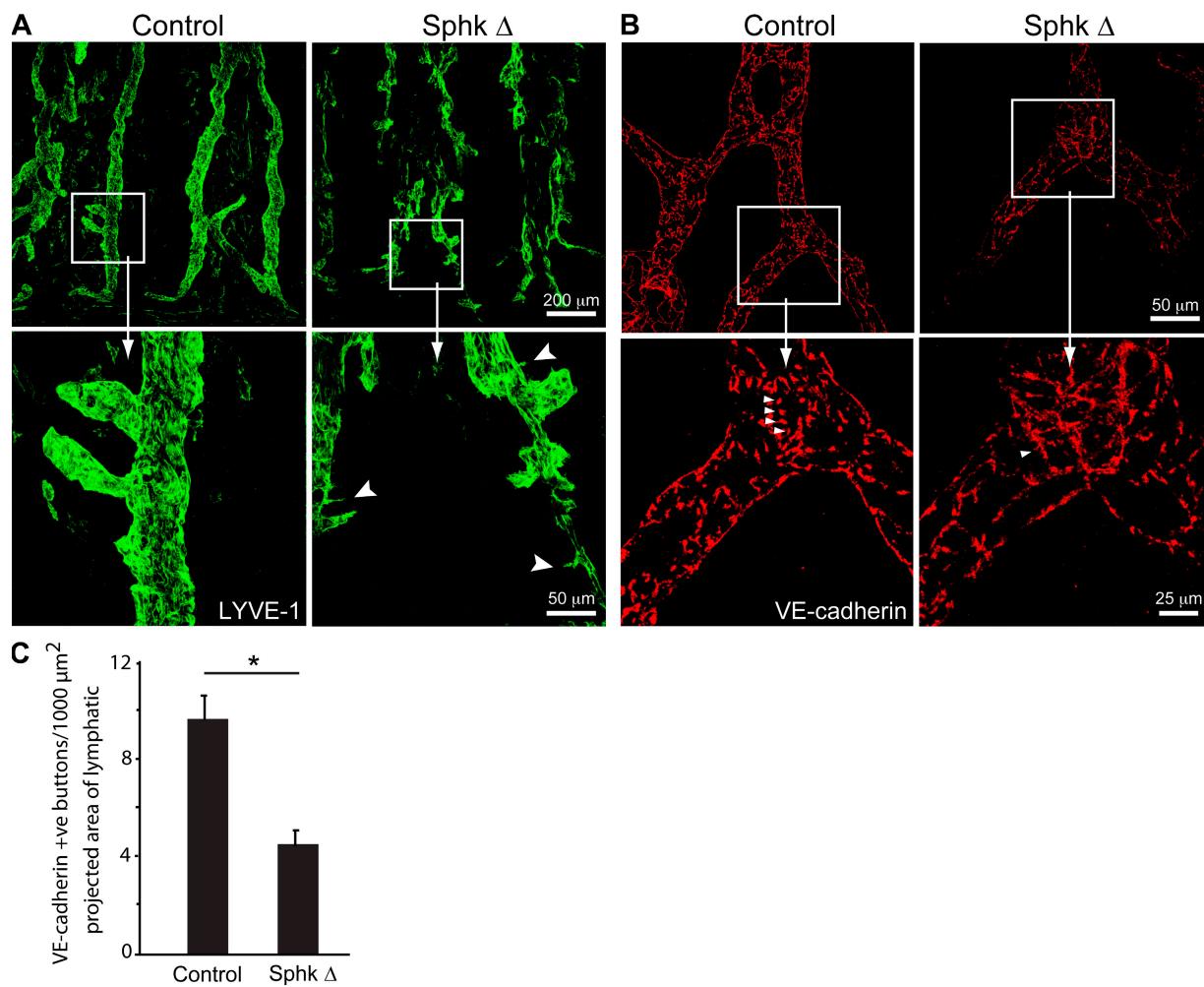
Figure 6. **Lymphatic *Sphk* expression is required for normal lymphatic vessel maturation.** (A) Confocal images showing lymphatic vessels stained with antibody against LYVE-1 in whole mount of mouse trachea. Arrowheads point to the jagged appearance of the lymphatic vessels in *Lyve-1 Cre+ Sphk*-deficient mice. (B) Confocal images showing the button-like pattern of VE-cadherin at endothelial cell–cell junctions of the diaphragm initial lymphatics. Arrowheads mark VE-cadherin+ buttons in the control and a corresponding junctional region in the *Lyve-1 Cre+ Sphk*-deficient mice. White squares (top) indicate enlarged regions (bottom). Data are representative of six experiments (n = 6 mice). (C) VE-cadherin buttons per 1,000-μm² projected area of lymphatic for littermate control and lymphatic Sphk-deficient trachea (n = 3 mice per group). Bars show means ± SE. *, P < 0.05 (Student's t test).

Lyve-1 Cre[+] *Sphk*-deficient and control mice. 2 d later, similar numbers of transferred DCs were recovered from the popliteal LNs of both types of mice (Fig. S4 G), suggesting that the afferent lymphatics of *Lyve-1 Cre*[+] *Sphk*-deficient mice can support DC migration.

Concluding remarks

Using a genetic approach, we provide evidence in this report that LECs are the main source of S1P needed for lymphocyte egress from LNs and Peyer's patches into lymph. The partial Lyve-1 Cre activity in BECs is considered unlikely to account for the reduction in lymph S1P because the amounts of S1P in blood were unaffected by Lyve-1 Cre-mediated *Sphk1* ablation. We also consider it unlikely that Lyve-1 Cre activity in hematopoietic cells is responsible, because the major hematopoietic cell populations were well replaced by wild-type cells in BM chimera experiments that showed no restoration in lymph S1P; involvement of some other cell type that was not tracked in our analysis and that had high Lyve-1 Cre activity and was not well replaced by irradiation and reconstitution with wild-type BM cannot be ruled out, but is considered the less likely explanation of our observations. The ability to restore measurable lymphocyte egress in lymphatic *Sphk*-deficient mice by antagonizing Gαi-mediated retention provided evidence that the egress defect was caused by a requirement for S1P to act on the lymphocytes rather than on endothelial egress barriers. These studies support a model in which S1P produced locally by LYVE-1^{+} cortical sinus lining cells is essential in promoting lymphocyte egress from LNs. In addition, lymphatic *Sphk*-deficient mice exhibit altered morphology and junctional patterning in initial lymphatic vessels in nonlymphoid tissues, establishing a role for Sphk activity, and likely S1P, in maturation of these vessels. The similar lack of cortical sinus lymphocytes in LNs from *Sphk*-deficient mice and 6-h FTY720-treated mice, together with the PTX treatment and DC migration data, suggests that the emptying of these sinuses is secondary to the block in lymphocyte egress rather than being a consequence of developmental abnormalities. However, we do not rule out the possibility that cortical sinus endothelial cell junctions are affected by *Sphk* deficiency. Finally, our findings suggest that perturbations altering S1P availability or S1P receptor function may lead to alterations in lymphatic vessels, and further work will be needed to define the extent to which such perturbations affect lymphatic function.

MATERIALS AND METHODS

Mice and adoptive cell transfer. CD45.2 C57BL/6 (B6) and CD45.1 B6 mice were from the National Cancer Institute or a colony maintained at the University of California, San Francisco. Mice lacking *Sphk2* and carrying *LoxP*-flanked *Sphk1* were on a B6/129 mixed background (Pappu et al., 2007). *Lyve-1 Cre* knockin mice on a B6/129 mixed background were generated as described in Fig. S1. *Lyve-1 Cre*[+] *Sphk1*[f/− or f/f] *Sphk2*^{−/−} mice were generated by intercrossing. Control mice were usually littermates and were always from the same intercross and carried at least one wild-type *Sphk* allele. Rosa26-YFP reporter mice (Srinivas et al., 2001) were provided by N. Killeen (University of California, San Francisco, San Francisco, CA). To generate BM chimeras, recipient CD45.2[+] mice were lethally irradiated with 1,300 rads in

two doses separated by 3 h and injected with 5×10^6 wild-type BM cells prepared from a CD45.1[+] donor. In some experiments, $\sim2 \times 10^7$ cells/ml were labeled with 3.3 µM CFSE (Invitrogen) or 10 µM 5-(and-6)-(((4-chloromethyl)benzoyl)amino)tetramethylrhodamine (CMTMR; Invitrogen) in RPMI 1640 containing 2% FCS for 20 min at 37°C, and were then washed by spinning through a layer of FCS. Labeled cells were resuspended at $\sim2 \times 10^7$ cells/ml, and were treated with 10 ng/ml OB or PTX at 37°C for 10 min, washed twice in warm RPMI 1640 with 2% FCS and 10 mM Hepes, and transferred to recipient mice. Lymph collection was performed as previously described (Matloubian et al., 2004). In brief, under a stereomicroscope, lymph was drawn from the cysterna chyli using a fine borosilicate glass microcapillary pipette (Sutter Instrument Co.). Cell numbers determined by flow cytometry were divided by the volume of collected lymph to determine the concentration. Protocols were approved by the Institutional Animal Care and Use Committee of the University of California, San Francisco.

Isolation of LECs. LNs removed from mice were minced into small pieces and added into RPMI 1640 medium containing 2% FCS, 10 mM Hepes, 100 µg/ml DNase, and 0.2 mg/ml Blendzyme 2 (Roche). The samples were incubated at 37°C for 25 min, rotating. Midway through the digestion, samples were passed through glass Pasteur pipettes multiple times to help break up the pieces of LNs. The digestion was stopped by addition of EDTA and FCS to a final concentration of 10 mM and 10%, respectively. The samples were filtered through 100-µM cell strainers and centrifuged at 450 *g* for 7 min. Cell pellets were resuspended in RPMI 1640 medium containing 2% FCS, 10 mM Hepes, and 5 mM EDTA for analysis.

S1P bioassay. The assay was performed as described by Pappu et. al. (2007). In brief, platelet-poor plasma or cell-depleted lymph was titrated into RPMI 1640 containing 10 mM Hepes and 0.5% fatty-acid free BSA (EMD) in a 96-well U-bottom plate. 4×10^4 WEHI231 cells stably expressing FLAG-tagged S1P1 (Lo et al., 2005) were added to each well, and the plate was incubated for 40 min at 37°C. Cells were analyzed by flow cytometry to measure the surface FLAG-S1P1 level using the M2-FLAG antibody (Sigma-Aldrich). Lymph was drawn as described in Mice and adoptive cell transfer into Alsever solution, and cells were removed by centrifugation. Platelet-poor plasma was prepared by centrifuging whole blood for 10 min at 630 *g* at room temperature.

Immunohistochemical and flow cytometric analysis. 7-µm cryostat sections were fixed and stained as previously described (Reif et al., 2002). CFSE-labeled cells were visualized in sections with alkaline phosphatase–conjugated antifluorescein antibodies (Roche). Congenic transferred lymphocytes were visualized by staining with biotinylated antibodies to CD45.1 (clone A20) or CD45.2 (clone 104). The LYVE-1–specific antibody Mab22 was generated as previously described (Pham et al., 2008) and was from R&D Systems. The anti–mouse gp38 (podoplanin) hybridoma was from American Type Culture Collection. For visualization of LYVE-1^{+} structures in sections, either unconjugated or biotinylated Mab22 was used. Lymphocyte preparations were stained with various fluorochrome-conjugated antibodies purchased from BD or anti-S1P1 as previously described (Lo et al., 2005), and data were acquired on a FACS LSRII (BD) and analyzed with FlowJo software (Tree Star, Inc.).

Immunofluorescence analysis. 7-µm sections were prepared from paraformaldehyde-fixed tissues, dried, and blocked with immunomix (1× PBS, 5% normal serum, 0.3% Triton X-100, 0.2% BSA, and 0.1% sodium azide) for at least 1 h. Sections were stained with primary antibodies in immunomix: biotinylated anti–LYVE-1 (R&D Systems) and rabbit anti-GFP (Invitrogen or Millipore) for 3 h to overnight. After two washes with 1× PBS, sections were stained with Cy3- and Cy5-conjugated antibodies (Jackson ImmunoResearch Laboratories, Inc.) and DAPI for 3 h. Sections were analyzed on a microscope (Axiovert Z1; Carl Zeiss, Inc.). For whole-mount staining, mice were perfused for 2 min with fixative (1% paraformaldehyde in PBS, pH 7.4) from a cannula inserted through the left ventricle into the aorta. The tracheas and diaphragms were removed and immersed in fixative

for 1 h at 4°C. Tissues were washed, stained with the antibodies described or anti–VE-cadherin (clone BV13), and viewed with a confocal microscope (LSM-510; Carl Zeiss, Inc.) as described previously (Baluk et al., 2007). Projection images were generated using AIM confocal software (version 3.2.2; Carl Zeiss, Inc.) from 10 consecutive frames, each 0.75 µm thick.

Online supplemental material. Fig. S1 shows a map of the *Lyve-1 EGFP-hCRE* construct and targeted locus. Fig. S2 shows the efficiency of *Lyve-1 Cre*-mediated gene deletion, effect on egress, and cortical sinus emptying after FTY720 treatment. Fig. S3 shows the recovery of B cell egress in *Lyve-1 Cre Sphk*-deficient mice by PTX treatment and cell distribution in LN cortical sinusoids. Fig. S4 shows the effect of *Sphk* deficiency on lymphatic vasculature. Online supplemental material is available at http://www.jem.org/cgi/content/full/jem.20091619/DC1.

REFERENCES

Azzali, G. 2003. Structure, lymphatic vascularization and lymphocyte migration in mucosa-associated lymphoid tissue. *Immunol. Rev.* 195:178–189. doi:10.1034/j.1600-065X.2003.00072.x

Baluk, P., T. Tammela, E. Ator, N. Lyubynska, M.G. Achen, D.J. Hicklin, M. Jeltsch, T.V. Petrova, B. Pytowski, S.A. Stacker, et al. 2005. Pathogenesis of persistent lymphatic vessel hyperplasia in chronic airway inflammation. *J. Clin. Invest.* 115:247–257.

Baluk, P., J. Fuxe, H. Hashizume, T. Romano, E. Lashnits, S. Butz, D. Vestweber, M. Corada, C. Molendini, E. Dejana, and D.M. McDonald. 2007. Functionally specialized junctions between endothelial cells of lymphatic vessels. *J. Exp. Med.* 204:2349–2362. doi:10.1084/jem.20062596

Camerer, E., J.B. Regard, I. Cornilissen, Y. Srinivasan, D.N. Duong, D. Palmer, T.H. Pham, J.S. Wong, R. Pappu, and S.R. Coughlin. 2009. Sphingosine-1-phosphate in the plasma compartment regulates basal and inflammation-induced vascular leak in mice. *J. Clin. Invest.* 119:1871–1879.

Gordon, E.J., N.W. Gale, and N.L. Harvey. 2008. Expression of the hyaluronan receptor LYVE-1 is not restricted to the lymphatic vasculature; LYVE-1 is also expressed on embryonic blood vessels. *Dev. Dyn.* 237:1901–1909. doi:10.1002/dvdy.21605

Grigorova, I.L., S.R. Schwab, T.G. Phan, T.H. Pham, T. Okada, and J.G. Cyster. 2009. Cortical sinus probing, S1P1-dependent entry and flow-based capture of egressing T cells. *Nat. Immunol.* 10:58–65. doi:10.1038/ni.1682

Jackson, D.G. 2004. Biology of the lymphatic marker LYVE-1 and applications in research into lymphatic trafficking and lymphangiogenesis. *APMIS.* 112:526–538. doi:10.1111/j.1600-0463.2004.apm11207-0811.x

Jakubzick, C., M. Bogunovic, A.J. Bonito, E.L. Kuan, M. Merad, and G.J. Randolph. 2008. Lymph-migrating, tissue-derived dendritic cells are minor constituents within steady-state lymph nodes. *J. Exp. Med.* 205:2839–2850. doi:10.1084/jem.20081430

Karpanen, T., and K. Alitalo. 2008. Molecular biology and pathology of lymphangiogenesis. *Annu. Rev. Pathol.* 3:367–397. doi:10.1146/annurev.pathmechdis.3.121806.151515

Kawahara, A., T. Nishi, Y. Hisano, H. Fukui, A. Yamaguchi, and N. Mochizuki. 2009. The sphingolipid transporter spns2 functions in migration of zebrafish myocardial precursors. *Science.* 323:524–527. doi:10.1126/science.1167449

Kennedy, S., K.A. Kane, N.J. Pyne, and S. Pyne. 2009. Targeting sphingosine-1-phosphate signalling for cardioprotection. *Curr. Opin. Pharmacol.* 9:194–201. doi:10.1016/j.coph.2008.11.002

Kono, M., M.L. Allende, and R.L. Proia. 2008. Sphingosine-1-phosphate regulation of mammalian development. *Biochim. Biophys. Acta.* 1781: 435–441.

Lee, M.J., S. Thangada, K.P. Claffey, N. Ancellin, C.H. Liu, M. Kluk, M. Volpi, R.I. Sha'afi, and T. Hla. 1999. Vascular endothelial cell adherens junction assembly and morphogenesis induced by sphingosine-1-phosphate. *Cell.* 99:301–312. doi:10.1016/S0092-8674(00)81661-X

Lee, J.F., Q. Zeng, H. Ozaki, L. Wang, A.R. Hand, T. Hla, E. Wang, and M.J. Lee. 2006. Dual roles of tight junction-associated protein, zonula occludens-1, in sphingosine 1-phosphate-mediated endothelial chemotaxis and barrier integrity. *J. Biol. Chem.* 281:29190–29200. doi:10.1074/jbc.M604310200

Link, A., T.K. Vogt, S. Favre, M.R. Britschgi, H. Acha-Orbea, B. Hinz, J.G. Cyster, and S.A. Luther. 2007. Fibroblastic reticular cells in lymph nodes regulate the homeostasis of naive T cells. *Nat. Immunol.* 8:1255–1265. doi:10.1038/ni1513

Lo, C.G., Y. Xu, R.L. Proia, and J.G. Cyster. 2005. Cyclical modulation of sphingosine-1-phosphate receptor 1 surface expression during lymphocyte recirculation and relationship to lymphoid organ transit. *J. Exp. Med.* 201:291–301. doi:10.1084/jem.20041509

Matloubian, M., C.G. Lo, G. Cinamon, M.J. Lesneski, Y. Xu, V. Brinkmann, M.L. Allende, R.L. Proia, and J.G. Cyster. 2004. Lymphocyte egress from thymus and peripheral lymphoid organs is dependent on S1P receptor 1. *Nature.* 427:355–360. doi:10.1038/nature02284

Mizugishi, K., T. Yamashita, A. Olivera, G.F. Miller, S. Spiegel, and R.L. Proia. 2005. Essential role for sphingosine kinases in neural and vascular development. *Mol. Cell. Biol.* 25:11113–11121. doi:10.1128/MCB.25.24.11113-11121.2005

Oliver, G., and R.S. Srinivasan. 2008. Lymphatic vasculature development: current concepts. *Ann. NY Acad. Sci.* 1131:75–81. doi:10.1196/annals.1413.006

Osborne, N., K. Brand-Arzamendi, E.A. Ober, S.W. Jin, H. Verkade, N.G. Holtzman, D. Yelon, and D.Y. Stainier. 2008. The spinster homolog, two of hearts, is required for sphingosine 1-phosphate signaling in zebrafish. *Curr. Biol.* 18:1882–1888. doi:10.1016/j.cub.2008.10.061

Paik, J.H., A. Skoura, S.S. Chae, A.E. Cowan, D.K. Han, R.L. Proia, and T. Hla. 2004. Sphingosine 1-phosphate receptor regulation of N-cadherin mediates vascular stabilization. *Genes Dev.* 18:2392–2403. doi:10.1101/gad.1227804

Pappu, R., S.R. Schwab, I. Cornelissen, J.P. Pereira, J.B. Regard, Y. Xu, E. Camerer, Y.W. Zheng, Y. Huang, J.G. Cyster, and S.R. Coughlin. 2007. Promotion of lymphocyte egress into blood and lymph by distinct sources of sphingosine-1-phosphate. *Science.* 316:295–298. doi:10.1126/science.1139221

Pfeiffer, F., V. Kumar, S. Butz, D. Vestweber, B.A. Imhof, J.V. Stein, and B. Engelhardt. 2008. Distinct molecular composition of blood and lymphatic vascular endothelial cell junctions establishes specific functional barriers within the peripheral lymph node. *Eur. J. Immunol.* 38:2142–2155. doi:10.1002/eji.200838140

Pham, T.H., T. Okada, M. Matloubian, C.G. Lo, and J.G. Cyster. 2008. S1P1 receptor signaling overrides retention mediated by G alpha i-coupled receptors to promote T cell egress. *Immunity.* 28:122–133. doi:10.1016/j.immuni.2007.11.017

Reif, K., E.H. Ekland, L. Ohl, H. Nakano, M. Lipp, R. Förster, and J.G. Cyster. 2002. Balanced responsiveness to chemoattractants from adjacent zones determines B-cell position. *Nature.* 416:94–99. doi:10.1038/416094a

Rosen, H., and E.J. Goetzl. 2005. Sphingosine 1-phosphate and its receptors: an autocrine and paracrine network. *Nat. Rev. Immunol.* 5:560–570. doi:10.1038/nri1650

Sanchez, T., T. Estrada-Hernandez, J.H. Paik, M.T. Wu, K. Venkataraman, V. Brinkmann, K. Claffey, and T. Hla. 2003. Phosphorylation and action of the immunomodulator FTY720 inhibits vascular endothelial cell growth factor-induced vascular permeability. *J. Biol. Chem.* 278:47281–47290. doi:10.1074/jbc.M306896200

Schwab, S.R., and J.G. Cyster. 2007. Finding a way out: lymphocyte egress from lymphoid organs. *Nat. Immunol.* 8:1295–1301. doi:10.1038/ni1545

Schwab, S.R., J.P. Pereira, M. Matloubian, Y. Xu, Y. Huang, and J.G. Cyster. 2005. Lymphocyte sequestration through S1P lyase inhibition and disruption of S1P gradients. *Science*. 309:1735–1739. doi:10.1126/science.1113640

Sinha, R.K., C. Park, I.Y. Hwang, M.D. Davis, and J.H. Kehrl. 2009. B lymphocytes exit lymph nodes through cortical lymphatic sinusoids by a mechanism independent of sphingosine-1-phosphate-mediated chemotaxis. *Immunity*. 30:434–446. doi:10.1016/j.immuni.2008.12.018

Srinivas, S., T. Watanabe, C.S. Lin, C.M. William, Y. Tanabe, T.M. Jessell, and F. Costantini. 2001. Cre reporter strains produced by targeted insertion of EYFP and ECFP into the ROSA26 locus. *BMC Dev. Biol*. 1:4. doi:10.1186/1471-213X-1-4

Venkataraman, K., Y.M. Lee, J. Michaud, S. Thangada, Y. Ai, H.L. Bonkovsky, N.S. Parikh, C. Habrukowich, and T. Hla. 2008. Vascular endothelium as a contributor of plasma sphingosine 1-phosphate. *Circ. Res*. 102:669–676. doi:10.1161/CIRCRESAHA.107.165845

Yoon, C.M., B.S. Hong, H.G. Moon, S. Lim, P.G. Suh, Y.K. Kim, C.B. Chae, and Y.S. Gho. 2008. Sphingosine-1-phosphate promotes lymphangiogenesis by stimulating S1P1/Gi/PLC/Ca2+ signaling pathways. *Blood*. 112:1129–1138. doi:10.1182/blood-2007-11-125203